

Published: August 31, 2022

**Citation:** Raveh Y, Nicolau-Raducu R, et al., 2022. The Elastic Constant of Coagulative Viscoelastometry, Medical Research Archives, [online] 10(8).

<https://doi.org/10.18103/mra.v10i8.3033>

Copyright: © 2022 European Society of Medicine. This is an open-access article distributed under the terms of the Creative Commons Attribution License, which permits unrestricted use, distribution, and reproduction in any medium, provided the original author and source are credited.

DOI

<https://doi.org/10.18103/mra.v10i8.3033>

ISSN: 2375-1924

## RESEARCH ARTICLE

# The Elastic Constant of Coagulative Viscoelastometry

**Yehuda Raveh MD<sup>\*1,2</sup>, Ramona Nicolau-Raducu MD, PhD<sup>1,2</sup>, Todd Smaka Todd MD BSME BSEE<sup>1</sup>, David Raveh<sup>3</sup>**

<sup>1</sup> Department of Anesthesia, University of Miami/Jackson Memorial Hospital, Miami, FL, USA

<sup>2</sup> Miami Transplant Institute, University of Miami/Jackson Memorial Hospital, Miami, FL, USA

<sup>3</sup> Student, Departments of Physics and Mathematics, University of Miami, Coral Gables, FL, USA

\*[yraveh@miami.edu](mailto:yraveh@miami.edu)

## ABSTRACT

Clot strength is of utmost clinical significance. The elastic constant of the forming clot is a surrogate of its strength. The elastometric assessment of the forming clot, known as thromboelastography, is therefore of utmost clinical importance. Thromboelastography using a rotational viscoelastometer requires a geometric model to couple the shear deformation of a forming blood clot to its viscoelastic properties. Hartert's original model idealized the complex geometry of the clot as a single cuboid and predicted a maximal effective shear modulus  $G_{max}=5000$  dyn/cm<sup>2</sup>. Hochleitner et al. recently reviewed this decades-old model, with the aim to refine it by reducing geometric simplifications that made the model more tractable. Hochleitner's revised model uncouples annular segments and idealizes them as cuboids, thereby obtaining a maximal effective shear modulus of  $G_{max}=4466$  dyn/cm<sup>2</sup>. Hochleitner's idealizations, while more accurate than Hartert's, still produces error of at least 52%. Using the actual formula for annular shear from an applied torque, as derived by Ramberg and Miller, obviates several geometric simplifications assumed for analytical tractability and produces an elastic constant of  $G=2930$  dyn/cm<sup>2</sup>. The clinical importance of precise determination of the formula for transforming clot amplitude to clot strength is underscored by the nonlinear relationship between elastometric amplitude and elastic constant, as the systematic error cannot be linearly rescaled. Thus, clot strength in several clinical scenarios should be based on clot strength as opposed to clot amplitude.

**Keywords:** Viscoelastometry, Thromboelastograph, Clot strength, Shear Modulus, Coagulation

## Abbreviations:

VEM, Viscoelastometer;

TEG, Thromboelastograph

## 1. | INTRODUCTION

Normal hemostasis controls exsanguination by rapidly sealing injured vessels with a blood clot that is strong enough to withstand the pressure and shear stress imposed by hemodynamic forces. Clot strength, therefore, is of utmost clinical importance. In 1948 Helmut Hartert designed a prototype viscoelastometer (VEM) that measures the forming clot strength and kinetics.<sup>1</sup> Of all contemporary clinical coagulation tests, elastometry provides the most comprehensive assessment of hemostasis. Consequently, viscoelastometry has become the standard of care in trauma, transplant, and cardiac anesthesia. Nevertheless, viscoelastometric quantification of clot strength continues to elude clinicians and researchers alike. In this manuscript we present the prevailing methodology and flaws of VEM-derived quantification of clot strength. We then derive more accurate formula for the conversion of amplitude to clot strength in clinical coagulative elastometry.

### 1.1 | Background

Viscoelastometry is the measurement of two distinct material properties: viscosity and elasticity. Viscosity describes the resistance of fluids to flow,<sup>2</sup> and elasticity is the physical property of a solid to return to its original shape and size upon removal of a deforming force.<sup>3</sup> Viscoelastic materials possess both fluid and solid properties. In contrast to the instantaneous response of solid materials, blood clots and many other biological materials

show gradual deformation and recovery in response to a transient deforming force. This time-dependent anelastic behavior of materials is called viscoelasticity.<sup>4</sup> VEMs apply a small and gradual force to the evolving blood clot; viscosity, therefore, is negligible and can be ignored.<sup>5-7</sup> As such, the clot can be viewed as an elastic solid that obeys linear elasticity.<sup>5-7</sup> Linearity denotes a direct proportionality between a deforming force and ensuing deformation, such as stretch, compression, twist (torsion), or shear (sliding). When a tangential (i.e. parallel and coplanar) shearing force ( $F$ ) is applied to a surface of an elastic cuboid with area ( $A$ ), it produces a shear stress equal to  $F/A$  (Figure 1), and results in a tangential displacement of area  $A$  by  $\Delta x$ . The tangential displacements of inner layers of the cuboid decrease monotonously toward the fixed layer. The shear strain is defined as the fractional deformation in the dimension ( $L$ ) along which the stress and strain spread, and equals  $\Delta x/L$  (Figure 1). The proportionality constant between shear stress to shear strain is called the shear modulus, and is denoted by  $G$ .<sup>3</sup> Accordingly, in a cuboid the shear modulus is

$$G = \frac{\text{Shear stress}}{\text{Shear strain}} = \frac{F/A}{\Delta x/L} = \frac{F \cdot L}{A \cdot \Delta x} \quad (1)$$

In the clinical arena, VEMs estimate the effective shear modulus  $G$  as a surrogate of clot strength; 'effective' shear modulus differs from standard definition of shear modulus in that it is an estimate that is derived from a model.

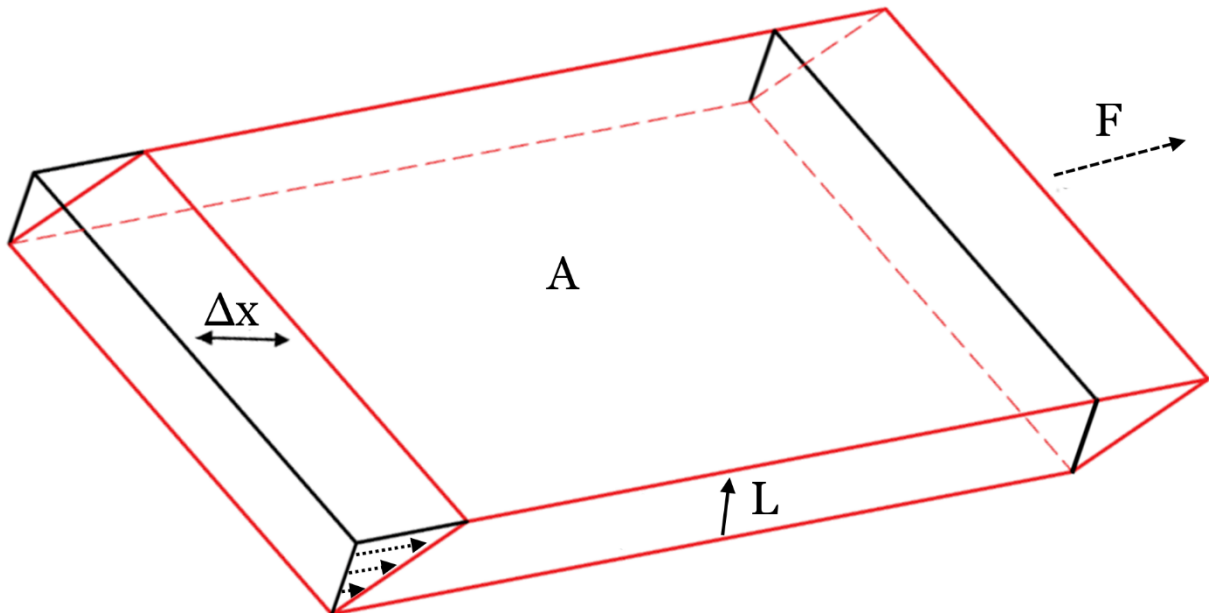


**Figure 1:** The shear modulus of a cuboid and an annulus.

A force  $F$  is shearing surface area  $A$  of the cuboid and deforms it by  $\Delta x$  in the direction of the force. The tangential displacements decrease monotonously in the inner layers of thickness  $L$  (black arrows). The shear modulus  $G$  is derived from the equation  $G = \frac{F/A}{\Delta x/L}$ . Adapted from Hochleitner et al.<sup>5</sup>

Hartert's apparatus included a cylindrical stainless-steel plunger, coaxially suspended on a

torsion wire inside a cylindrical stainless-steel cup (Figure 2A).<sup>5</sup> A fresh sample of blood is placed in the cup and coagulation is initiated. As the nascent clot adheres to the inner surface of the cup and the outer surface of the plunger, the clot assumes the irregular geometry of the space between the cup and the plunger. This space can be divided into two vertical cylindrical segments and an inverted conical base (Figure 2B).<sup>5</sup>

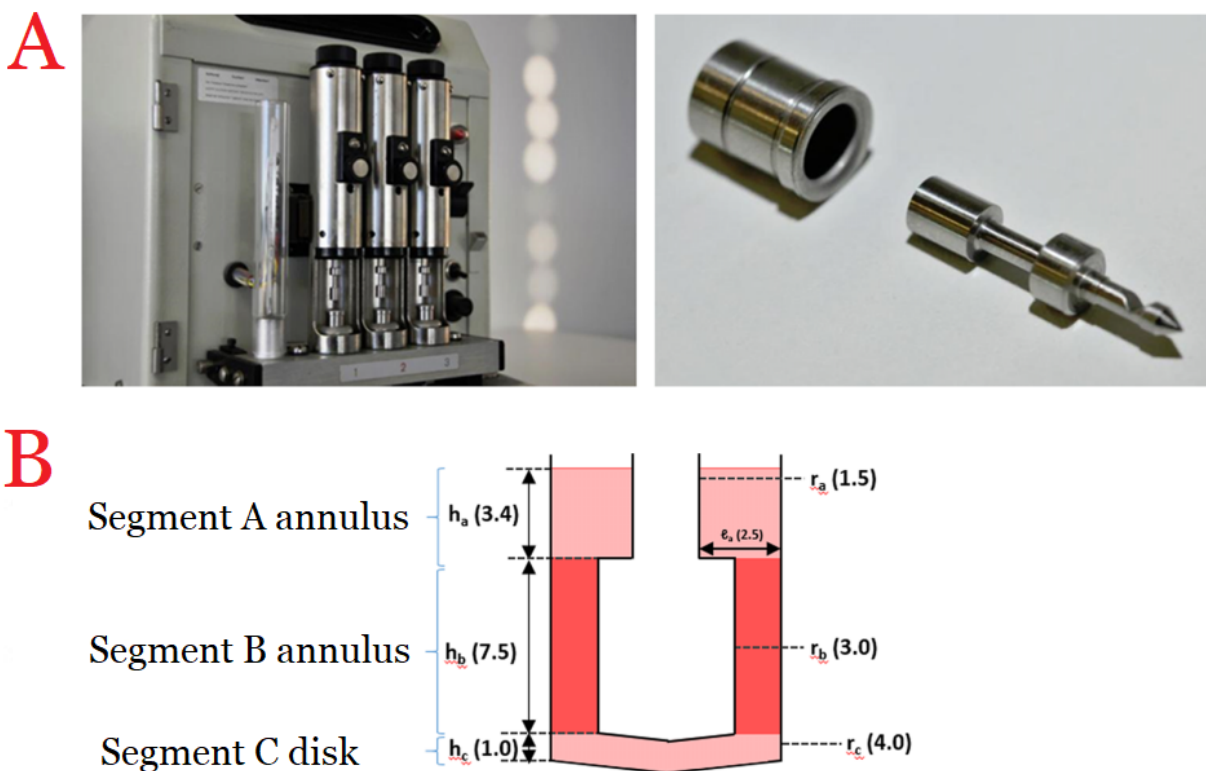


**Figure 2:** Hartert's Thromboelastograph.

Panel (A): Hartert's prototype viscoelastometer (left) includes a cylindrical stainless-steel plunger, coaxially suspended on a torsion wire inside a cylindrical stainless steel cup.

Panel (B): After fresh sample of blood is placed in the cup and activation of coagulation, the nascent clot assumes the irregular geometry of the space between the cup and the plunger with two vertical cylinders (segments A and B), and an inverted conical base (segment C). Adapted from Hochleitner et al.<sup>5</sup>

The cup oscillates by  $\theta' = 1/24$  radian in each direction,<sup>7</sup> and applies a torque, i.e. a rotational force, on the outer layers of the two cylindrical clot segments, as well as the base. The torque spreads centripetally (cylindrical segments A and B) and upwards (conical base, i.e., segment C; Figure 2B) and the shear stress and strain ultimately reach the innermost layer of the clot. As depicted in panels A and B of Figure 3, the resultant shear stress that acts on these three segments angularly displaces their outer and inner layers by  $\theta'$  and  $\theta$ , respectively. At the completion of each half oscillation the cup comes to a stand-still. This pause is sufficiently long for all

layers of the clot and the plunger to come to a rotational stand-still, and a short steady state is achieved.<sup>7</sup> During this steady state, the torques acting on concentric clot's layers equalize, and all layers of the clot become immobile. In the innermost layer of the clot, a tangential force ( $F$ ) produces a torque ( $T$ ) that rotates the plunger and wire, so that  $T = F*r$ , where  $r$  is the distance between  $F$  and the perpendicular radius ( $r$ ) of rotation of the plunger (Figure 3A). The torsional stiffness ( $\tau$ ) of the wire hinders its twisting;  $\tau$  is defined as the torque required to twist the wire by one radian. The torque, therefore, also equals  $\tau*\theta$ . Taken together,

$T = F \cdot r = \tau \cdot \theta$ , and after rearrangement:  $F = \frac{\tau \cdot \theta}{r}$ .  
As the torsional wire arrests the plunger's rotation at  $\theta$ , the innermost clot's layer becomes fixed, and relative to it the outermost layer is angularly displaced by a magnitude of  $\theta' - \theta$  (Figure 3 A & B).

As with a cuboid, the angular displacements of the inner layers of a clot formed in Hartert's thromboelastograph (TEG) decrease monotonously toward the plunger (Figure 3B).

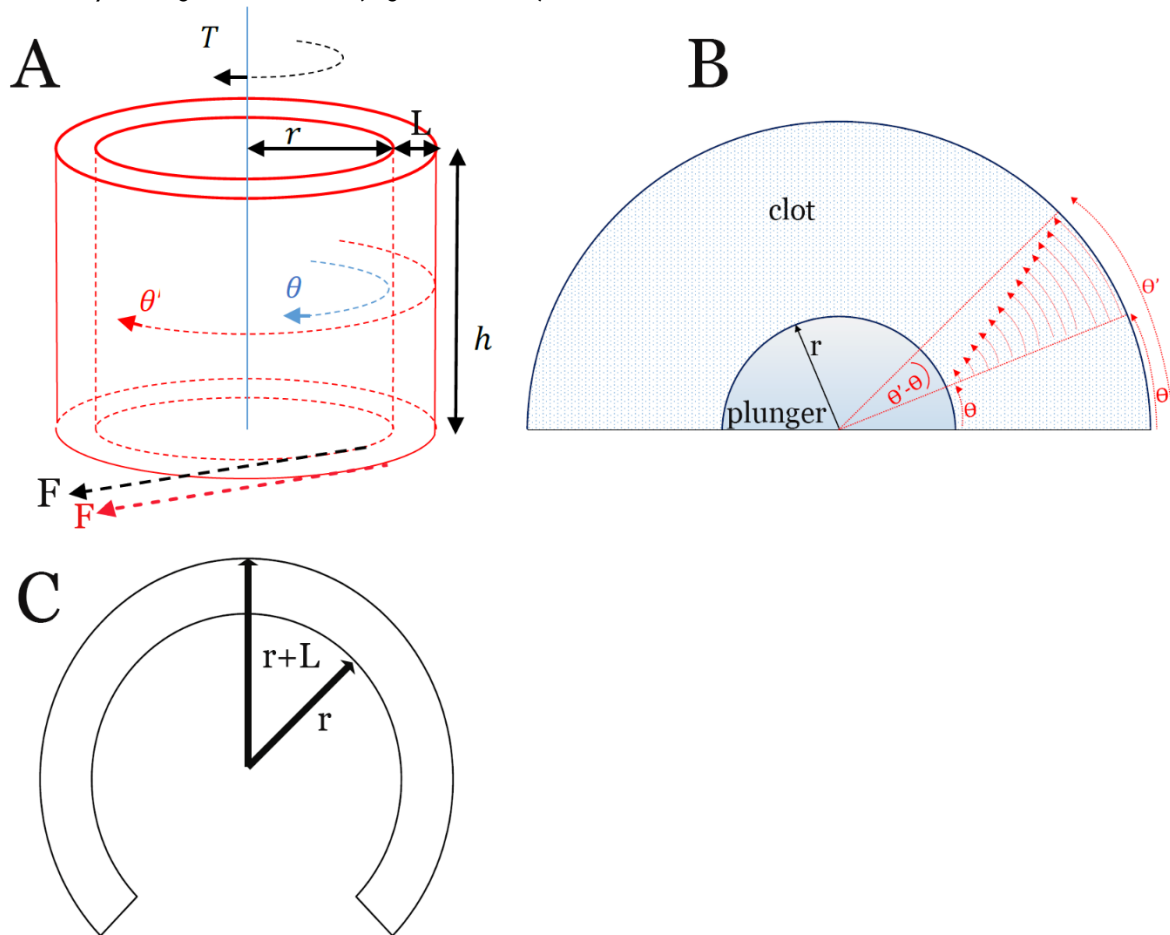


**Figure 3:** The shear modulus of an annulus in Hartert's apparatus.

Panel (A): The cylindrical outermost clot layer of an annular segment in Hartert's thromboelastograph is attached to the cup and oscillates with it by angle  $\theta'$ . The innermost layer is attached to the plunger. The innermost layer has an angular displacement of  $\theta$  and imposes a torque ( $T$ ) on the plunger. Adapted from Hochleitner et al.<sup>5</sup>

Panel (B). Hartert's apparatus includes a plunger suspended on a torsion wire inside a blood-filled cylindrical cup. The cup oscillates by  $\theta'$  radians and applies a torque on the outer layers of the clot. The torque spreads centripetally and upwards and ultimately reaches the innermost layer of the clot, which then begins to rotate the plunger. As the torsional wire arrests the plunger's rotation at  $\theta$ , the innermost clot's layer becomes fixed, and relative to it the outermost layer is angularly displaced by a magnitude of  $\theta' - \theta$ . Ensuing angular displacements of the inner layers decrease monotonously toward the plunger.

Panel (C): Unfolding a cylinder along its long-axis yields a horseshoe-shaped object that cannot be straightened due to uneven inner and outer curvatures.

## 2.0 | The Shear Modulus of Hartert's TEG

In 1962, Hartert formulated the derivation of the shear modulus in his apparatus.<sup>7</sup> In the absence of a tool for precise analysis, and for the sake of

tractability, Hartert restricted his calculation to the longer cylinder alone (Segment B of Figure 2B). He visualized the annular clot as if sliced along its long (vertical) axis and unwrapped (Figure 3C); the

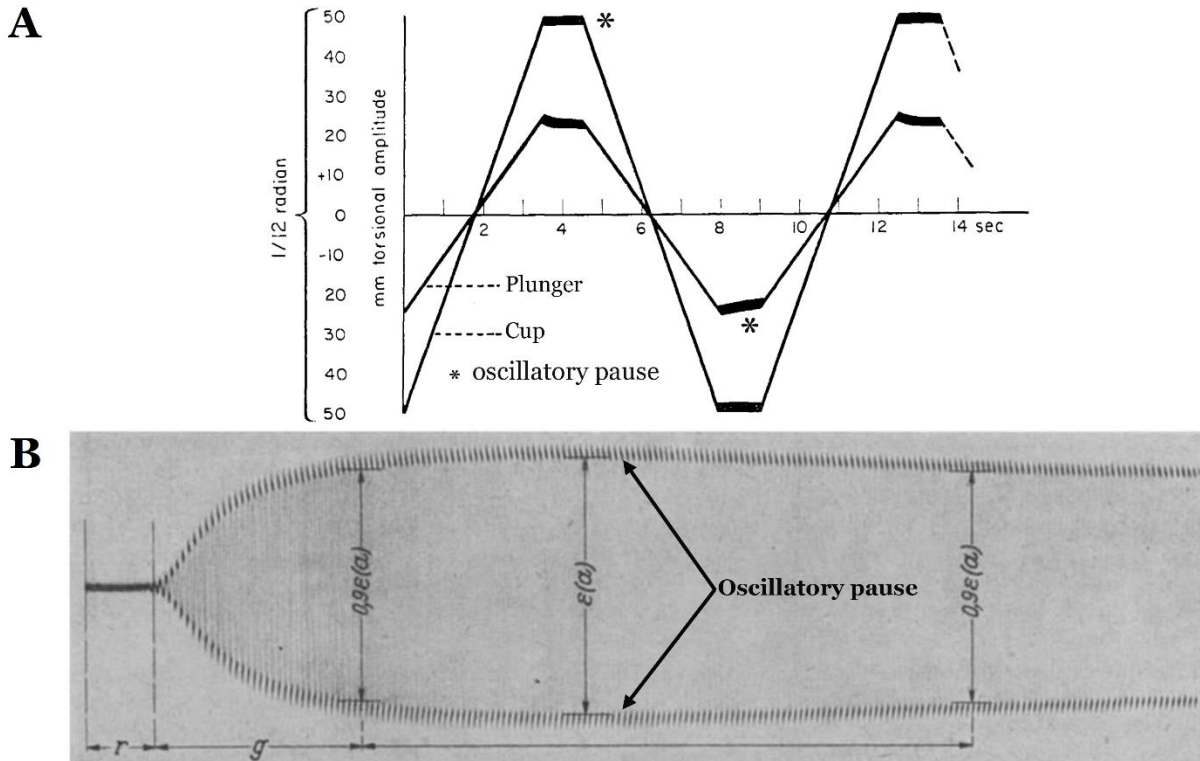
resultant annular shape has two concentric curves whose arc lengths ratio equals the ratio of their radii. For tractability, however, Hartert idealized the annulus as a sheared cuboid with an area  $A=2\pi hr$  and an ensuing linear displacement of

$$G = \frac{F \cdot L}{A \cdot \Delta x} = \frac{L \cdot \tau \cdot \theta}{2\pi hr \cdot r \cdot (\theta' - \theta)} = \frac{L\tau}{2\pi hr^3} \cdot \frac{\theta}{(\theta' - \theta)} \quad (2)$$

Experimenting with healthy individuals' blood, Hartert observed a maximal inner displacement  $\theta$  of  $\theta_{\max} = \theta' / 2$ , and after rearrangement  $2\theta_{\max} = \theta'$ . For this maximal displacement and with his apparatus variables' values, Hartert calculated an effective maximal shear modulus  $G_{\max} = \frac{L \cdot \tau \cdot \theta}{2\pi hr \cdot r \cdot (2\theta - \theta)} = \frac{L\tau}{2\pi hr^3} = 5000 \text{ dyn/cm}^2$ , and referred to  $G_{\max}$  as the (elastic) constant of TEG.<sup>5,7</sup> Hartert's graphing apparatus was calibrated so that a full cup oscillation of  $2\theta' = 1/12$  radians

$\Delta x = r \cdot (\theta' - \theta)$ , where  $h$  and  $r$  are the height and inner radius of the clot annulus, respectively (Figure 3A). After substitution for  $A$ ,  $F$  and  $\Delta x$  in Eq. (1), we get:

corresponded to 100 mm deflection on the graphing paper,<sup>7</sup> while the total (back and forth) angular amplitude of the plunger ( $2\theta$ ) was recorded as linear deflection ( $S$  in mm) for each oscillation (supplementary Figure 4A). An actual recording of Hartert's TEG is given in Supplementary Figure 4B.<sup>5,7</sup> Accordingly, contemporary TEG commonly transforms an angular amplitude into an effective shear modulus by the formula  $G = 5000 \cdot \frac{S}{(100 - S)}$ <sup>8,9</sup>



**Supplementary Figure 4:** Recording of the oscillatory motion of Hartert's thromboelastograph.

Panel (A): Schematic representation of cup and plunger's oscillatory angular motions in radians and corresponding graphically-recorded linear displacements in mm, after reaching maximum clot strength of normal blood. Adapted from Hartert.<sup>7</sup>

Panel (B): Actual recording of Hartert's thromboelastograph. Amplitude of the angular motion, in mm, is depicted along the y-axis of a film paper moving leftward along the x-axis in at a speed of 2 mm/min. Adapted from Hartert.<sup>1</sup>

## 2.1 | The shear modulus of an annular elastic body.

In 1953, nine years before Hartert's analysis and presumably unbeknownst to Hartert, using

$$G = \frac{T}{4\pi h(\theta' - \theta)} * \left( \frac{1}{r^2} - \frac{1}{(r+L)^2} \right) = \frac{\tau\theta}{4\pi h(\theta' - \theta)} * \left( \frac{1}{r^2} - \frac{1}{(r+L)^2} \right). \quad (3)$$

Equation (3) was later described by Brannon as well.<sup>11</sup> The error ( $\varepsilon$ ) associated with employing Eq. (2) in lieu of Eq. (3) depends on the ratio  $q = \frac{L}{r}$  as follow:

$\varepsilon = \frac{2q^2+3q}{2+q}$  (please see supplementary file 1, section A for derivation). Given that segment B in Hartert's design had dimensions of  $L_b = 0.1$  cm and  $r_b = 0.3$  cm,  $q = \frac{1}{3}$ , the error  $\varepsilon = \frac{2q^2+3q}{2+q} = \frac{11}{21} = 0.52$ . Thus, by idealizing segment B as a cuboid, Hartert overestimated its clot firmness by 52%. For a  $\leq 5\%$  error, the  $\frac{L}{r}$  ratio should be  $\leq 0.0332$  (supplementary file 1). In Hartert's apparatus, the  $\frac{L}{r}$  ratio was 10 times larger; thus, Hartert's visualization of the unwrapped annulus as a cuboid was unsound. Again, Hartert was presumably unaware of Ramberg and Miller's derivation of Eq. (3). It is valid, however, to idealize an annulus as a cuboid when the  $L \ll r$ , since Ramberg and Miller's equation then becomes identical to Hartert's equation, as shown in section B of supplementary file 1.

## 3.0 | Previous scrutiny of Hartert's calculations.

In 2017, Hochleitner et al. proposed a more refined calculation of the effective maximal shear modulus in Hartert's apparatus by including all three segments of the clot (Figure 2B).<sup>5</sup> Confronted with an object of irregular geometry, and lacking an exact analytical solution to the elasticity problem at hand, Hochleitner et al. did not seek the aid of available analytical tools. Instead, their approach was to: (i) separate the clot into three uncoupled segments, (ii) analyze each segment independently of its adjacent segment(s), and (iii) add the elastic resistance of all three segments to calculate the maximal effective stiffness of the clot (i.e.  $G_{max}$ ). Such an approach underestimates the effective clot stiffness and ignores the forces between adjacent layers, with ensuing geometric compatibility errors (please see Sections 3.1 and 3.2 below). Furthermore, in the calculation of the elastic resistance of the annular segments A and B, the authors did not use the governing annular equation (Eq. (3)) as derived decades earlier by Ramberg

and Miller.<sup>10,11</sup> Instead, and in common with Hartert, they idealized the annular segments as cuboids, which we above proved is only valid for  $L \ll r$ . While their error in idealizing segment B as a cuboid is identical to Hartert's, the now-included segment A has a ratio  $\frac{L}{r}$  of  $\frac{0.25}{0.15} = \frac{5}{3}$ , which yields an error  $\varepsilon = \frac{2q^2+3q}{2+q} = \frac{95}{33} = 2.88$ , i.e. 288% in excess of its true elastic resistance. Even so, the inclusion of segments A and C in the calculations more than canceled the overestimation of the elastic resistance of segment A (please see Section 3.1 below). Hochleitner calculated for the clot in its entirety an effective  $G_{max} = 4466$  dyn/cm<sup>2</sup>; a value that is nearly 11% lower than that calculated by Hartert.

## 3.1 | The impact of inclusion of additional clot's segments on calculated $G_{max}$

How the inclusion of additional clot's segments (segments A and C; Figure 2B) reduced the calculated effective stiffness could be intuitively appreciated as follows: The clot's resistance to torsional deformation is identical to a spring's resistance to stretch; a torque imposed on several clot's segments is, therefore, analogous to a force acting on several springs in parallel arrangement. The effective stiffness of a parallel arrangement of springs is the sum of the individual springs' stiffness,<sup>12</sup> and a given torque imposed on two parallel annuli of an elastic material would displace them less than when imposed on a single annulus. If we experimentally observe that a given torque imposed on two annuli of material "A" yields a displacement identical to the displacement recorded for a single annulus of material "B", we must conclude that the shear modulus ( $G$ ), i.e. the resistance, of material "A" is lower than that of material "B". As noted in Section 2.0, for tractability Hartert assumed that the clot's elastic resistance is due to segment B alone and calculated its  $G_{max}$  using a given torque and displacement. Hochleitner's analysis correctly used the same torque and displacement, and correctly attributed it to the elastic resistance of all three segments. As a result, Hochleitner calculated a smaller  $G_{max}$  by the virtue of inclusion of additional segments. The reduction in the effective elastic modulus  $G$ , when

attributed to 3 clot segments in parallel surpassed the overestimation of elastic resistance of segments A, to the extent that Hochleitner's calculated value was nearly 11% lower than that calculated by Hartert.

### 3.2 | Uncoupling of clot segments results in geometric incompatibilities.

Hochleitner's uncoupling of the clot segments results in geometric compatibility errors as follows: In response to a small stress, adjacent points of an intact material are expected to displace in conjunction with each other, and undergo nearly identical displacement, because internal forces resist the pulling-apart of the points. Hochleitner's methodology separated the continuous structural components of the clot, applied a shear force on each segment individually, and then summed up the

ensuing shear stresses and strains.<sup>5</sup> When considered independently, adjacent points of connected components may be predicted to deform incompatibly, i.e. with very different amplitudes. Figure 5 displays a schematic of the area near the horizontal surface of the plunger (the "shoulder"). Points A, A', A'' and B', B'' are on the clot's annular segments A and B, respectively. Points A'' and B'' are angularly displaced by  $\theta'$  while points A and B' are displaced by  $\theta < \theta'$ . The angular displacement of clots' layers in between A-A'' and B'-B'' of segment A and B, respectively, decreases monotonously in centripetal direction from  $\theta'$  to  $\theta$ , as shown in Figure 3B. Accordingly, in segments A and B the magnitudes of angular displacements are:  $A = \theta < A' < A'' = \theta'$ , and  $B' = \theta < B'' = \theta'$ , respectively.

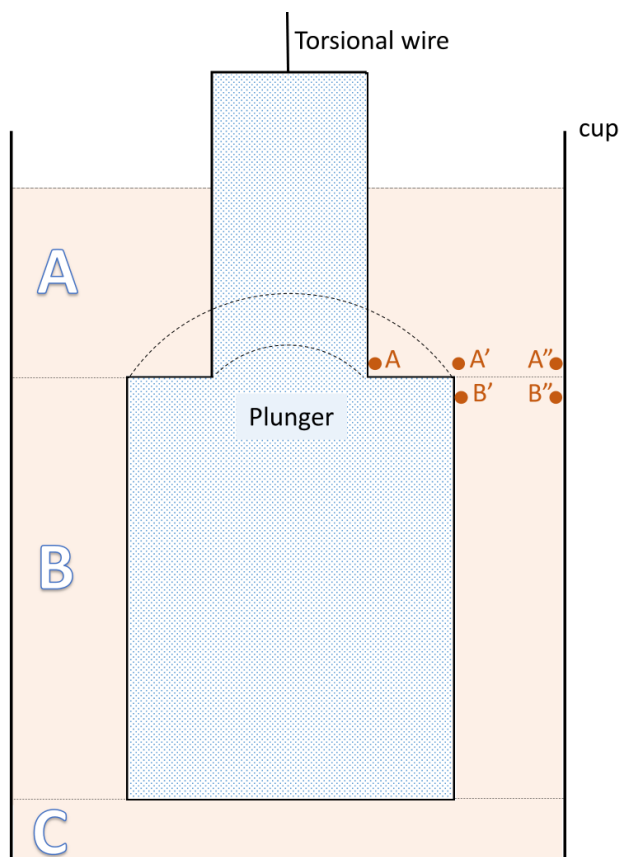


**Figure 5:** Geometric incompatibilities due to uncoupling of clot's segments.

The upper portion of the cup includes the attachment of segment A annulus to the horizontal "shoulder" of the plunger and to segment B annulus. The adjacent points A' and B' undergo nearly identical displacement, since internal forces resist the pulling apart of the points. When segments A and B are uncoupled and independently considered, these adjacent points are predicted to deform incompatibly, with very different amplitudes. In segments A and B the magnitudes of angular displacements are:  $A = \theta < A' < A'' = \theta'$ , and  $B' = \theta < B'' = \theta'$ , respectively. Thus, magnitudes of angular displacements are  $A = B' = \theta < A' < A'' = B'' = \theta'$ , with  $B' < A'$ . Uncoupling segments A and B results in a serious incompatibility since the contiguous points A' and B' deform compatibly with magnitudes  $A' \approx B'$ .

Combining these two orders of angular displacements' magnitudes yields  $A = B' = \theta < A' < A'' = B'' = \theta'$ , with  $B' < A'$ . But the adjacent points  $A'$  and  $B'$  are expected to undergo nearly identical angular displacement, i.e.  $A' \approx B'$ . Simply put, uncoupling segments A and B frees the contiguous points  $A'$  and  $B'$  to deform unrestrictedly and with magnitudes  $B' < A'$ , when in fact  $A' \approx B'$ . Thus the untethering of the adjacent points  $A'$  and  $B'$  results in a serious incompatibility. The internal forces between segments further restrict their displacement and enhance the effective elastic resistance. In addition, the attachment of segment A to the horizontal surface of the plunger (the "shoulder") adds additional elastic resistance to the displacement of the clot, but this too was intentionally unaccounted for by Hochleitner's analysis, for the sake of tractability. Similar to added resistance driven by the inclusion of additional clot segments, added resistance due to attachment of segment A to the plunger's shoulder and the attachment of clot segments to each other should further decrease the calculated effective  $G_{max}$  for a given  $\theta$ . Thus, accounting for the errors associated with idealizing the two annuli as cuboids is insufficient, and the true shear modulus is expected to be even lower.

#### 4.0 | Recalculation of $G_{max}$ using Ramberg and Miller equation.

Hochleitner et al.'s inclusion of all 3 clot's segments proffered a more precise method for estimating  $G_{max}$ . The accuracy of Hochleitner's approach could be further increased by using Ramberg and Miller's equation to estimate the contribution of annular segments A and B to total  $G_{max}$  of Hartert's clot. From Eq. (3) the elastic resistance of an annulus is

$$G = \frac{T}{4\pi h(\theta' - \theta)} * \left( \frac{1}{r^2} - \frac{1}{(r+L)^2} \right) \quad \text{and} \quad \text{after rearrangement } T = \frac{G4\pi h(\theta' - \theta)}{\left( \frac{1}{r^2} - \frac{1}{(r+L)^2} \right)}$$

From Hochleitner's derivation the torque of segment C—the conical base—is  $T_c = \frac{G2\pi(\theta' - \theta)r_b^4}{4h_c}$ .

The total torque on the clot is the sum of its three components so that  $T_{total} = T_a + T_b + T_c$ . But the total torque also equals the torque on the torsional wire so that  $T_{total} = \tau\theta$  and  $\tau\theta = T_a + T_b + T_c = \frac{G4\pi h_a(\theta' - \theta)}{\left( \frac{1}{r_a^2} - \frac{1}{(r_a+L_a)^2} \right)} + \frac{G4\pi h_b(\theta' - \theta)}{\left( \frac{1}{r_b^2} - \frac{1}{(r_b+L_b)^2} \right)} + \frac{G2\pi(\theta' - \theta)r_b^4}{4h_c}$ .

Hartert and Hochleitner papers <sup>5,7</sup> provided the following values:  $h_a = 0.3352$  cm;  $r_a = 0.15$  cm;  $L_a = 0.25$  cm;  $h_b = 0.75$  cm;  $r_b = 0.3$  cm;  $L_b = 0.1$  cm;  $h_c = 0.1$  cm;  $\tau = 6377$  dyn/cm; and  $(\theta' - \theta) = \theta$  as derived from Hartert's observation.

$$6377 = \frac{G4\pi 0.3352}{\left( \frac{1}{0.15^2} - \frac{1}{(0.15+0.25)^2} \right)} + \frac{G4\pi 0.75}{\left( \frac{1}{0.3^2} - \frac{1}{(0.3+0.1)^2} \right)} + \frac{G2\pi 0.3^4}{4*0.1} = \frac{G4\pi 0.3352}{38.1944} + \frac{G4\pi 0.75}{4.8611} + \frac{G2\pi 0.0081}{0.4} = 0.11028G + 1.9388G + 0.12723G = 2.1763G, \text{ and } G = 2930 \frac{\text{dyn}}{\text{cm}^2}$$

#### 4.0 | DISCUSSION

Algorithms for transfusion of blood products and administration of hemostatic agents incorporate VEM-derived clot-kinetics and maximal clot strength variables into clinical decision-making.<sup>13,14</sup> VEMs, therefore, require accurate calibration of calculated clot strength. For several decades the calibration of VEMs has proven challenging due to complex clot geometry that lacks an analytical elasticity solution. The flaws of published methodologies largely stem from the need to separate the clot to simpler geometric shapes, and presumable unfamiliarity with the 1953 derivation of the governing equation of shear modulus of an annulus by Ramberg and Miller.<sup>10</sup> In this regard, our calculations offer a highly improved precision by addressing the latter alone. Accordingly, Hartert's and Hochleitner's values have over-estimation errors of at least 70.6% and 52.4%, respectively. The actual elastic constant of normal blood is

expectedly lower than 2930 dyn/cm<sup>2</sup> due to resistive forces between the clot segments and the attachment to the plunger's horizontal shoulder, as discussed in section 3.2.

Some have argued that since thromboelastographic determination of  $G$  is inherently insufficiently accurate, it may be preferable to use a dimensionless linearity constant between clot elasticity and amplitude.<sup>5</sup> The premise is that for clinical decisions recorded values are compared to manufacturer-provided reference values, regardless of VEM-provided absolute value.<sup>5</sup> However,  $G$  reflects clot strength and in several clinical scenarios decisions should be based on clot strength as opposed to clot amplitude due to the nonlinear relationship between clot strength and amplitude.<sup>15</sup> The improved accuracy of VEM-derived clot stiffness is, therefore, of paramount clinical importance.

A superior VEM-calibration methodology would be to use the VEM machine to measure the shear modulus of an elastic material of a known shear modulus, and with elastic properties—such as Young's modulus and Poisson ratio—similar to blood. A comparison of the VEM-derived shear modulus with the material's known elastic constants would then yield the calibration/conversion factor of amplitude to  $G$ . This methodology, however, is likely to be costly due to damage to the cup and plunger.

Hartert's notion that VEM amplitude can be transformed into clot elasticity was based on the premise that viscosity's contribution to clot strain is negligible. However, Hartert's supposition was later challenged by the VEMs recording of substantial strain amplitudes in experiments where blood was substituted with liquids of sufficiently high shear viscosity, despite the absence of fluid elasticity.<sup>16-18</sup>

Determination of the viscoelastic constant of a VEM clot of irregular shapes may be more readily achieved with innovative, up-to-date rheological methods, such as finite elemental analysis, ultrasonic

shear-wave approach, quartz crystal microbalance assay, and surface plasmon resonance.<sup>19-23</sup> These contemporary rheological methods also permit an independent measurement of clot's viscosity and elasticity and the related shear-loss and shear-storage moduli.

#### 4.1 Limitations and Conclusions

The calculations in this study specifically apply to Hartert's TEG. Despite increased accuracy, our calculation of the elastic constant of coagulative elastometry overestimates the actual value due to some residual and inevitable simplifications. An up-to-date rheological methodology should be implemented to derive the actual viscosity and elasticity constants of coagulative elastometry.

#### Acknowledgment

The authors thank John M. Maloney, Ph.D., Massachusetts Institute of Technology, Department of Materials Science and Engineering for his expertise and assistance in all aspects of the study, and for critical review of the manuscript.

## References

1. Hartert H. Blutgerinnungsstudien mit der Thrombelastographie; einem neuen Untersuchungsverfahren [Blood clotting studies with Thrombus stressography; a new investigation procedure]. *Klin Wochenschr.* Oct 1 1948;26(37-38):577-83. Blutgerinnungsstudien mit der Thrombelastographie; einem neuen Untersuchungsverfahren. doi:10.1007/BF01697545
2. Özkaya N, Nordin M, Goldsheyder D, Leger D. Mechanical Properties of Biological Tissues. *Fundamentals of Biomechanics*. Springer, New York, NY; 2012:221-236: Chapter 15.
3. Elert G. The Physics Hypertextbook. Elasticity Accessed March 10th, 2022. <https://physics.info/elasticity/>
4. Capurro M, Barberis F. Evaluating the mechanical properties of biomaterials. In: Dubruel P, Van Vlierberghe S, eds. *Biomaterials for Bone Regeneration*. Woodhead Publishing; 2014:270-323:chap 9.
5. Hochleitner G, Sutor K, Levett C, Leyser H, Schlimp CJ, Solomon C. Revisiting Hartert's 1962 Calculation of the Physical Constants of Thrombelastography. *Clin Appl Thromb Hemost.* Apr 2017;23(3):201-210. doi:10.1177/1076029615606531
6. Hartert H. Thrombelastography: physical and physiological aspects. In: Copley AL SG, ed. *Flow Properties of Blood and Other Biological Systems*. Pergamon Press; 1960:186-196.
7. Hartert H, Schaefer JA. The physical and biological constants of thrombelastography. *Biorheology.* 1962;1(1):31-39. doi:10.3233/bir-1962-1105
8. Chandler WL. The thromboelastography and the thromboelastograph technique. *Semin Thromb Hemost.* 1995;21 Suppl 4:1-6. <https://www.ncbi.nlm.nih.gov/pubmed/8747681>
9. Haemoscope Corporation. *PN06-510 TEG 5000 User Manual*. Haemoscope Corporation; 2007. <https://studylib.net/doc/18643089/pn06-510-teg-5000-user-manual>
10. Ramberg W, Miller JA. Stress-Strain Relation in Shear From Twisting Test of Annulus. *J Res Nat Bur Stands.* 1953; 50:125-130 doi:<http://dx.doi.org/10.6028/jres.050.019>
11. Brannon R. Annulus Twist as a verification test. March 10th, 2022, 2022. Updated 09/01/2011. Accessed 09/15, 2020. <https://csmbrannon.net/author/rebeccabrannon/>
12. Weggel DC, Boyajian DM, Chen S-E. Modelling structures as systems of springs. *World Transactions on Engineering and Technology Education.* 2007;6(1):169-172. [http://www.wiete.com.au/journals/WTE&TE/Pages/TOC\\_V6N1.html](http://www.wiete.com.au/journals/WTE&TE/Pages/TOC_V6N1.html)
13. Baksaas-Aasen K, Gall L, Eaglestone S, et al. iTACTIC - implementing Treatment Algorithms for the Correction of Trauma-Induced Coagulopathy: study protocol for a multicentre, randomised controlled trial. *Trials.* 2017;18(1):486-486. doi:10.1186/s13063-017-2224-9
14. Sakai T. Viscoelastic testing in liver transplantation. *Transfusion.* Oct 2020;60 Suppl 6(S6):S61-S69. doi:10.1111/trf.16077
15. Solomon C, Ranucci M, Hochleitner G, Schöchl H, Schlimp CJ. Assessing the Methodology for Calculating Platelet Contribution to Clot Strength (Platelet Component) in Thromboelastometry and Thrombelastography. *Anesth Analg.* 2015;121(4):868-878. doi:10.1213/ANE.0000000000000859
16. Evans PA, Hawkins K, Lawrence M, et al. Rheometry and associated techniques for blood coagulation studies. *Med Eng Phys.* Jul 2008;30(6):671-9. doi:10.1016/j.medengphy.2007.08.005
17. Scott Blair GW, Burnett J. On the rates of coagulation and subsequent softening of bovine and human blood and of thrombin-fibrinogen. *Biorheology.* 1968;5:163-176. doi:10.3233/BIR-1968-5207
18. Scott Blair GW, Burnett J. Thrombelastography of Newtonian fluids. *Biorheology.* 1968;5:177-177. doi:10.3233/BIR-1968-5208
19. Huang CC, Chen PY, Shih CC. Estimating the viscoelastic modulus of a thrombus using an ultrasonic shear-wave approach. *Med Phys.* Apr 2013;40(4):042901. doi:10.1118/1.4794493
20. Scogin T, Yesudasan S, Walker MLR, Averett RD. Electromagnetically Induced Distortion of a Fibrin Matrix with Embedded Microparticles. *J Mech Med Biol.* 2018;18:1850016. doi:10.1142/S0219519418500161
21. Tutwiler V, Singh J, Litvinov RI, Bassani JL, Purohit PK, Weisel JW. Rupture of blood clots: Mechanics and pathophysiology. *Sci Adv.* Aug 2020;6(35):eabc0496. doi:10.1126/sciadv.abc0496
22. Oberfrank S, Drechsel H, Sinn S, Northoff H, Gehring FK. Utilisation of Quartz Crystal Microbalance Sensors with Dissipation (QCM-D) for a Clauss Fibrinogen Assay in Comparison with Common Coagulation Reference Methods. *Sensors*

(Basel). 2016;16(3):282-282.

doi:10.3390/s16030282

23. Vikinge TP, Hansson KM, Benesch J, et al. Blood plasma coagulation studied by surface plasmon resonance. *J Biomed Opt.* Jan 2000;5(1):51-5. doi:10.1117/1.429968 DOI: 10.1117/1.429968.